

Mass-splittings of doubly heavy baryons in QCD

R.M. Albuquerque^{a,b,1}, S. Narison^{b,*}

^a Instituto de Física, Universidade de São Paulo, C.P. 66318, 05389-970 São Paulo, SP, Brazil.

^b Laboratoire de Physique Théorique et Astroparticules, CNRS-IN2P3 & Université de Montpellier II, Case 070, Place Eugène Bataillon, 34095 - Montpellier Cedex 05, France.

Abstract

We consider (for the first time) the ratios of doubly heavy baryon masses (spin 3/2 over spin 1/2 and SU(3) mass-splittings) using double ratios of sum rules (DRSR), which are more accurate than the usual simple ratios often used in the literature for getting the hadron masses. In general, our results agree and compete in precision with potential model predictions. In our approach, the α_s corrections induced by the anomalous dimensions of the correlators are the main sources of the $\Xi_{QQ}^* - \Xi_{QQ}$ mass-splittings, which seem to indicate a $1/M_Q$ behaviour and can only allow the electromagnetic decay $\Xi_{QQ}^* \rightarrow \Xi_{QQ} + \gamma$ but not to $\Xi_{QQ} + \pi$. Our results also show that the SU(3) mass-splittings are (almost) independent of the spin of the baryons and behave approximately like $1/M_Q$, which could be understood from the QCD expressions of the corresponding two-point correlator. Our results can be improved by including radiative corrections to the SU(3) breaking terms and can be tested, in the near future, at Tevatron and LHCb.

Keywords: QCD spectral sum rules, baryon spectroscopy, heavy quarks.

1. Introduction

In a previous paper [1], we have considered, using double ratios [2–6] of QCD spectral sum rules (QSSR) [7, 8] (DRSR), the splittings due to SU(3) breakings of the baryons made with one heavy quark. In this paper, we pursue this project in the case of doubly heavy baryons. The absolute values of the doubly heavy baryon masses of spin 1/2 ($\Xi_{QQ} \equiv QQ\bar{u}$) and spin 3/2 ($\Xi_{QQ}^* \equiv QQ\bar{u}$) have been obtained using QCD spectral sum rules (QSSR) (for the first time) in [9] with the results in GeV:

$$\begin{aligned} M_{\Xi_{cc}^*}(3/2) &= 3.58(5), & M_{\Xi_{bb}^*}(3/2) &= 10.33(1.09), \\ M_{\Xi_{cc}}(1/2) &= 3.48(6), & M_{\Xi_{bb}}(3/2) &= 9.94(91), \end{aligned} \quad (1)$$

and in [10]:

$$M_{\Xi_{bcu}} = 6.86(28). \quad (2)$$

More recently [11, 12], some results have been obtained using some particular choices of the interpolating currents. The predictions for $M_{\Xi_{cc}^*}$ and $M_{\Xi_{cc}}$ are in good agreement with the experimental candidate $M_{\Xi_{cc}} = 3518.9$ [13]. We shall also improve these previous predictions by working with the DRSR for estimating the mass ratio of the 3/2 over the 1/2 baryons and shall compare them with some potential model predictions [10, 14–16].

2. The interpolating currents and the two-point correlator

For the spin 1/2 $QQ\bar{q}$ baryons, and following Ref. [9], we work with the lowest dimension currents:

$$J_{\Xi_Q} = \epsilon_{\alpha\beta\lambda} \left[(Q_a^T C \gamma_5 q_\beta) + b(Q_a^T C q_\beta) \gamma_5 \right] Q_\lambda, \quad (3)$$

where $q \equiv d, s$ are light quark fields, $Q \equiv c, b$ are heavy quark fields, b is *a priori* an arbitrary mixing parameter. Using the b -stability criterion of the QSSR results for the masses and couplings, the optimal values of these observables have been found for:

$$b = -1/5, \quad (4)$$

in the case of light baryons [17] and in the range [1, 18–20]:

$$-0.5 \leq b \leq 0.5, \quad (5)$$

for non-strange heavy baryons. The corresponding two-point correlator reads:

$$\begin{aligned} S(q) &= i \int d^4x e^{iqx} \langle 0 | \mathcal{T} \bar{J}_{\Xi_Q}(x) J_{\Xi_Q}(0) | 0 \rangle \\ &\equiv \hat{q} F_1 + F_2, \end{aligned} \quad (6)$$

where²: $\hat{q} \equiv q$. The invariants F_j ($j = 1, 2$) obey the dispersion relation:

$$F_j(q^2) = \int_{(2M_Q+mq)^2}^{\infty} \frac{dt}{t - q^2 - i\epsilon} \frac{1}{\pi} \text{Im} F_j(t) + \dots, \quad (7)$$

where ... indicate subtraction constants and $-q^2 \equiv Q^2 > 0$.

For the spin 3/2 $QQ\bar{q}$ baryons, we also follow Ref. [9] and work with the interpolating currents:

$$J_{\Xi_Q^*}^\mu = \sqrt{\frac{1}{3}} \epsilon_{\alpha\beta\lambda} \left[2(Q_a^T C \gamma^\mu d_\beta) Q_\lambda + (Q_a^T C \gamma^\mu Q_\beta) q_\lambda \right] \quad (8)$$

²We use the notation in the Landau and Lifchitz's book.

*Corresponding author

Email addresses: rma@if.usp.br (R.M. Albuquerque), snarison@yahoo.fr (S. Narison)

¹FAPESP thesis fellow within the France-Brazil bilateral exchange program.

The corresponding two-point correlator reads:

$$\begin{aligned} S^{\mu\nu}(q) &= i \int d^4x e^{iqx} \langle 0 | \mathcal{T} \bar{J}_{\Xi_Q^*}^\mu(x) J_{\Xi_Q^*}^\nu(0) | 0 \rangle \\ &\equiv g^{\mu\nu} (\hat{q} F_1 + F_2) + \dots, \end{aligned} \quad (9)$$

3. The two-point correlator in QCD

The expressions of the two-point correlator using the previous interpolating currents have been obtained in the chiral limit $m_q = 0$ and including the mixed condensate contributions by [9]. In this paper, we extend these results by including the linear strange quark mass corrections to the perturbative and $\langle \bar{s}s \rangle$ condensate contributions. We shall use the same normalizations as in [9].

For the spin 1/2 baryons, these corrections read:

$$\begin{aligned} \text{Im} F_1^{m_s}|_{\text{pert}} &= \frac{3m_s m_Q^3}{2^8 \pi^3} (1 - b^2) \left[6\mathcal{L}_v(2x^2 - 1) \right. \\ &\quad \left. + v \left(6x + 1 + \frac{2}{x} \right) \right], \\ \text{Im} F_2^{m_s}|_{\text{pert}} &= \frac{m_s m_Q^4}{2^9 \pi^3} \left[12\mathcal{L}_v \left[2x(5b^2 + 2b + 5) \right. \right. \\ &\quad \left. \left. - 3(3b^2 + 2b + 3) \right] + \right. \\ &\quad \left. v \left[12(5b^2 + 2b + 5) \right. \right. \\ &\quad \left. \left. + \frac{4}{x}(5b^2 + 8b + 5) + \frac{1}{x^2}(1 - b)^2 \right] \right], \\ \text{Im} F_1^{m_s}|_{\bar{s}s} &= \frac{m_s \langle \bar{s}s \rangle}{2^8 \pi} \left[v \left[7b^2 + 4b + 7 + \right. \right. \\ &\quad \left. \left. 8(b^2 + b + 1)x \right] + \frac{3}{v}(1 + b^2) \right], \\ \text{Im} F_2^{m_s}|_{\bar{s}s} &= 3 \frac{m_s m_Q \langle \bar{s}s \rangle}{2^7 \pi} (1 - b^2) \left(3v + \frac{1}{v} \right). \end{aligned} \quad (10)$$

For the spin 3/2 baryons, these corrections read:

$$\begin{aligned} \text{Im} F_1^{m_s}|_{\text{pert}} &= \frac{m_s m_Q^3}{24 \pi^3 x} \left[6\mathcal{L}_v(2x^2 - 1)x + \right. \\ &\quad \left. v(6x^2 + x + 2) \right], \\ \text{Im} F_2^{m_s}|_{\text{pert}} &= \frac{m_s m_Q^4}{192 \pi^3 x^2} \left[24\mathcal{L}_v(x^2 + 6x - 5)x^2 + \right. \\ &\quad \left. v(12x^3 + 74x^2 + 10x + 3) \right], \\ \text{Im} F_1^{m_s}|_{\bar{s}s} &= -\frac{m_s \langle \bar{s}s \rangle}{96 \pi} \left[v(4x - 3) - \frac{5}{v} \right], \\ \text{Im} F_2^{m_s}|_{\bar{s}s} &= -\frac{m_s m_Q \langle \bar{s}s \rangle}{6 \pi v} (2x - 1), \end{aligned} \quad (11)$$

with:

$$x \equiv \frac{m_Q^2}{t}, \quad v \equiv \sqrt{1 - 4x}, \quad \mathcal{L}_v \equiv \log \left(\frac{1 + v}{1 - v} \right), \quad (12)$$

4. Form of the sum rules and QCD inputs

We shall work with the exponential sum rules [7, 24, 25]:

$$\mathcal{F}_i(\tau) = \int_{t_q}^{\infty} dt e^{-t\tau} \frac{1}{\pi} \text{Im} F_i(t), \quad (i = 1, 2), \quad (13)$$

($\tau \equiv 1/M^2$ is the sum rule variable) from which, one can derive the following ratios:

$$\begin{aligned} \mathcal{R}_i^q(\tau) &\equiv -\frac{d}{d\tau} \ln \mathcal{F}_i = \frac{\int_{t_q}^{\infty} dt t e^{-t\tau} \text{Im} F_i(t)}{\int_{t_q}^{\infty} dt e^{-t\tau} \text{Im} F_i(t)}, \quad (i = 1, 2), \\ \mathcal{R}_{21}^q(\tau) &\equiv \frac{\mathcal{F}_2}{\mathcal{F}_1} = \frac{\int_{t_q}^{\infty} dt e^{-t\tau} \text{Im} F_2(t)}{\int_{t_q}^{\infty} dt e^{-t\tau} \text{Im} F_1(t)}, \end{aligned} \quad (14)$$

used in the sum rule literature for extracting the baryon masses. We parametrize the spectral function using the standard duality ansatz: “one resonance”+ “QCD continuum”. The QCD continuum starts from a threshold t_c and comes from the discontinuity of the QCD diagrams, which is consistent with a matching of the QCD and the experimental sides of the sum rules for large t . The value of t_c is not arbitrary as its value obtained inside the region of t_c -stability of the sum rule is correlated to the ground state mass and coupling [21]. This simple duality model has been successfully tested in the literature when a complete data for the spectral functions are available, like e.g., e^+e^- to $I=1$ hadrons or to charmonium data [8]³. Transferring the QCD continuum contribution to the QCD side of the sum rules, one obtains the finite energy inverse Laplace sum rules:

$$\begin{aligned} |\lambda_{B_q^{(*)}}|^2 M_{B_q^{(*)}} e^{-M_{B_q^{(*)}}^2 \tau} &= \int_{t_q}^{t_c} dt e^{-t\tau} \frac{1}{\pi} \text{Im} F_2(t), \\ |\lambda_{B_q^*}|^2 e^{-M_{B_q^*}^2 \tau} &= \int_{t_q}^{t_c} dt e^{-t\tau} \frac{1}{\pi} \text{Im} F_1(t), \end{aligned} \quad (15)$$

where $\lambda_{B_q^{(*)}}$ and $M_{B_q^{(*)}}$ are the heavy baryon residue and mass from which one can derive the FESR analogue of the ratios of sum rules. Consistently, we also take into account the SU(3) breaking at the continuum threshold⁴:

$$\sqrt{t_c}|_{SU(3)} \simeq \left(\sqrt{t_c}|_{SU(2)} \equiv \sqrt{t_c} \right) + \bar{m}_s. \quad (16)$$

\bar{m}_s is the running strange quark mass. As we do an expansion in m_s , we take the threshold $t_q = 4m_Q^2$ for consistency. m_Q is the heavy quark mass, which we shall take in the range covered by

³More involved parametrizations of the continuum can also be proposed (see e.g. [22] for non-resonant final states within ChPT or [23] for a t -dependent t_c model). However, it is easy to check in the harmonic oscillator model discussed in [23] that the 5% uncertainties induced e.g. by a t -dependent continuum model on the ratio of moments will be negligible in the double ratio of sum rule (DRSR) defined in Eq. (20) as the leading corrections coming from light-quark flavour-independent terms will largely cancel out. This cancellation of the QCD continuum contribution will be signaled by the large range of t_c -stability region obtained in our analysis.

⁴As we have done an expansion in terms of m_s , the quark threshold has to be taken at $4m_Q^2$ but not at $(2m_Q + m_s)^2$.

the running and on-shell mass (see Table 1) because of its ambiguous definition when working to LO. At the τ -stability point of the FESR analogue of the ratios of sum rules, one obtains:

$$M_{B_q^{(*)}} \simeq \sqrt{\mathcal{R}_i^q} \simeq \mathcal{R}_{21}^q, \quad (i = 1, 2). \quad (17)$$

These predictions lead to a typical uncertainty of 10-15% [9, 19, 20], which are not competitive compared with predictions from some other approaches, especially from potential models [14]. In order to improve the QSSR predictions, we work with the double ratios of finite energy sum rules (DRSR)⁵:

$$r_i^{sd} \equiv \sqrt{\frac{\mathcal{R}_i^s}{\mathcal{R}_i^d}} \quad (i = 1, 2); \quad r_{21}^{sd} \equiv \frac{\mathcal{R}_{21}^s}{\mathcal{R}_{21}^d}. \quad (18)$$

which take directly into account the SU(3) breaking effects. These quantities are obviously less sensitive to the choice of the heavy quark masses and to the value of the continuum threshold than the simple ratios \mathcal{R}_i and \mathcal{R}_{21} ⁶. For the numerical analysis we shall introduce the RGI quantities \hat{m} and \hat{m}_q [26]:

$$\begin{aligned} \bar{m}_q(\tau) &= \frac{\hat{m}_q}{(-\log \sqrt{\tau}\Lambda)^{2/\beta_1}} \\ \langle \bar{q}q \rangle(\tau) &= -\hat{\mu}_q^3 (-\log \sqrt{\tau}\Lambda)^{2/\beta_1} \\ \langle \bar{q}Gq \rangle(\tau) &= -\hat{\mu}_q^3 (-\log \sqrt{\tau}\Lambda)^{1/\beta_1} M_0^2, \end{aligned} \quad (19)$$

where $\beta_1 = -(1/2)(11 - 2n/3)$ is the first coefficient of the β function for n flavours. We have used the quark mass and condensate anomalous dimensions reviewed in [8]. We shall use the QCD parameters in Table 1:

– We shall not include the $1/q^2$ term discussed in [27, 28], which is consistent with the LO approximation used here as the latter has been motivated for a phenomenological parametrization of the larger order terms of the QCD series.

– We have used the value of $\kappa \equiv \langle \bar{s}s \rangle / \langle \bar{d}d \rangle$ from [1] which we consider as improvements of the ones from light meson systems [8, 29–31], where the one from the scalar channel suffers from the unknown nature of the κ meson, while the one from the pseudoscalar channel depends on the theoretical appreciation of the π' meson contribution into the spectral function [8, 22]. However, the different estimates agree each others within the errors. To be conservative, we have multiplied the original error in [1] by 2.

– For the gluon condensate, we have used the estimate from heavy quarkonia and e^+e^- data [21, 24, 32–37]. We do not expect that the estimate from τ -decays is reliable as its contribution acquires an extra- α_s term in the τ width compared

to the one in the two-point correlator [38], while its value, in this process, can also be affected by the treatments of the large order PT series [27, 32]. However, the effect of the gluon condensate is not important in our analysis of the SU(3) breaking as it disappears like some other flavour-independent contributions in the DRSR.

– For the heavy quark masses, we use the range spanned by the running \overline{MS} mass $\overline{m}_Q(M_Q)$ and the on-shell mass from QSSR compiled in page 602, 603 of the book in [8].

Table 1: QCD input parameters. The values of Λ , \hat{m}_s and μ_d have been obtained from $\alpha_s(M_\tau) = 0.325(8)$ [32] and from the running masses: $\overline{m}_s(2) = 96.1(4.8)$ MeV and $\overline{m}_d(2) = 5.1(2)$ MeV [29]. The original errors for κ and $\langle \alpha_s G^2 \rangle$ have been multiplied by 2.

Parameters	Values	Ref.
$\Lambda(n_f = 4)$	(324 ± 15) MeV	[13, 32]
$\Lambda(n_f = 5)$	(194 ± 10) MeV	[13, 32]
\hat{m}_s	(114.5 ± 20.8) MeV	[6, 8, 13, 29]
$\hat{\mu}_d$	(263 ± 7) MeV	[8, 29]
$\kappa \equiv \langle \bar{s}s \rangle / \langle \bar{d}d \rangle$	(0.74 ± 0.06)	[1, 8, 29, 31]
M_0^2	(0.8 ± 0.1) GeV ²	[3, 17, 39]
$\langle \alpha_s G^2 \rangle$	$(6 \pm 2) \times 10^{-2}$ GeV ⁴	[21, 24, 32–37]
m_c	$(1.26 \sim 1.47)$ GeV	[8, 13, 29, 37, 40]
m_b	$(4.22 \sim 4.72)$ GeV	[8, 13, 29, 37, 40]

5. The Ξ_{QQ}^*/Ξ_{QQ} mass ratio

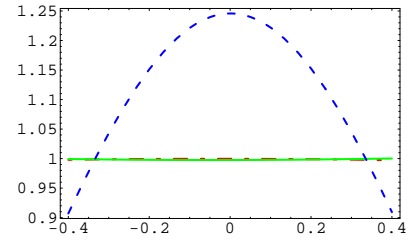


Figure 1: **Charm quark:** b -behaviour of the different DRSR given $\tau = 0.8$ GeV⁻² and $t_c = 25$ GeV². $r_1^{3/1}$ dot-dashed line (red); $r_2^{3/1}$ continuous line (green); $r_{12}^{3/1}$ dashed line (blue). We have used $m_c = 1.26$ GeV and the other QCD parameters in Table 1.

We extract the mass ratio using the DRSR analogue of the one in Eq. (18) which we denote by:

$$r_i^{3/1} \equiv \sqrt{\frac{\mathcal{R}_i^3}{\mathcal{R}_i^1}} : i = 1, 2; \quad r_{21}^{3/1} \equiv \frac{\mathcal{R}_{21}^3}{\mathcal{R}_{21}^1}, \quad (20)$$

where the upper indices 3 and 1 correspond respectively to the spin 3/2 and 1/2 channels. We use the QCD expressions of the two-point correlators given by [9] which we have checked. We notice like [9] that the mixed quark condensate contribution has a term which behaves like $1/v^3$ (where v is the heavy quark velocity), which signals a coulombic correction and would require a complete treatment of the non-relativistic coulombic corrections which is beyond the aim of this paper. Therefore, in our analysis, we truncate the QCD series at the dimension-4 condensates until which we have calculated the m_s corrections. We

⁵Analogous DRSR quantities have been used successfully (for the first time) in [3] for studying the mass ratio of the $0^{++}/0^{-+}$ and $1^{++}/1^{--}$ B-mesons, in [4] for extracting f_{B_s}/f_{B^*} , in [5] for estimating the $D \rightarrow K/D \rightarrow \pi$ semi-leptonic form factors and in [6] for extracting the strange quark mass from the $e^+e^- \rightarrow I = 1, 0$ data.

⁶One may also work with the double ratio of moments \mathcal{M}_n based on different derivatives at $q^2 = 0$ [3]. However, in this case the OPE is expressed as an expansion in $1/m_Q$, which for a LO expression of the QCD correlator is more affected by the definition of the heavy quark mass to be used.

shall only include the effect of the mixed condensate (if necessary) for controlling the accuracy of the approach or for improving the τ or/and t_c stability of the analysis.

The charm quark channel to lowest order in α_s

Fixing $\tau = 0.8 \text{ GeV}^{-2}$ and $t_c = 25 \text{ GeV}^2$, which are inside the τ - and t_c -stability regions (see Figs. 2 and 3), we show in Fig. 1 the b -behaviour of $r_i^{3/1}$ which shows that $r_1^{3/1}$ and $r_2^{3/1}$ are very stable but not $r_{12}^{3/1}$. We then disfavour $r_{12}^{3/1}$. Some common solutions are obtained for:

$$b \simeq -0.35, \quad \text{and} \quad b \simeq +0.2, \quad (21)$$

which are inside the range given in Eq. (5). For definiteness, we fix $b = -0.35$ (the other value $b = 0.2$ gives the same result) and study the τ -dependence of the result in Fig. 2. We have checked in Fig. 2b that the inclusion of the mixed condensate contribution does not affect the result from $r_i^{3/1}$ ($i = 1, 2$) obtained by retaining only the dimension-4 condensates (Fig. 2a) but affects the one from $r_{12}^{3/1}$. Therefore, we shall only retain the results from $r_i^{3/1}$ ($i = 1, 2$) and show their t_c -dependence in Fig. 3. The large stability in t_c confirms our expectation of the weak

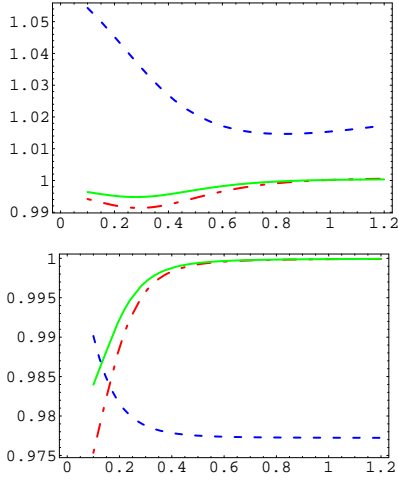


Figure 2: **Charm quark:** a) τ -behaviour of $r_1^{3/1}$: dot-dashed line (red), $r_2^{3/1}$: continuous line (green) and $r_{12}^{3/1}$ dashed line (blue) with $b = -0.35$ and $t_c = 25 \text{ GeV}^2$. b) the same as a) but when the mixed condensate is included.

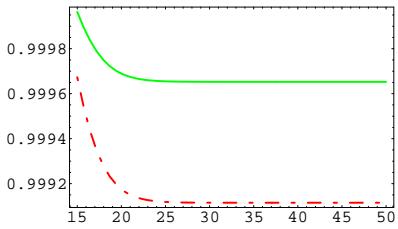


Figure 3: **Charm quark:** t_c -behaviour of $r_1^{3/1}$: dot-dashed line (red) and $r_2^{3/1}$: continuous line (green) with $b = -0.35$ and $\tau = 0.8 \text{ GeV}^{-2}$.

t_c -dependence of the DRSR and then on the non-sensitivity of the results on the exact form of the QCD continuum including an eventual slight t -dependence of t_c advocated in [23]. In these figures, we have used $m_c = 1.26 \text{ GeV}$. We have also checked that the results are insensitive to the change of the charm mass

to $m_c = 1.47 \text{ GeV}$. From these previous analysis, we deduce to lowest order from $r_i^{3/1}$ ($i = 1, 2$):

$$\frac{M_{\Xi_{cc}^*}}{M_{\Xi_{cc}}} = 0.9994(3). \quad (22)$$

The tiny error is the quadratic sum due to $\langle \alpha_s G^2 \rangle$, m_c and α_s .

The bottom quark channel to lowest order in α_s

We extend the analysis to the case of the bottom quark.

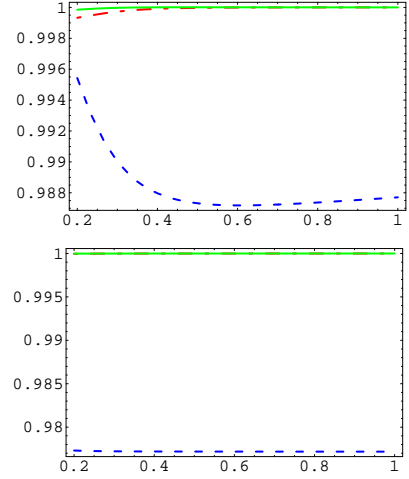


Figure 4: **Bottom quark:** a) τ -behaviour of $r_1^{3/1}$: dot-dashed line (red), $r_2^{3/1}$: continuous line (green) and $r_{12}^{3/1}$: dashed line (blue) with $b = -0.35$ and $t_c = 100 \text{ GeV}^2$; b) the same as a) but when the mixed condensate is included into the OPE.

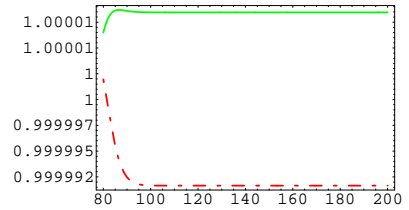


Figure 5: **Bottom quark:** t_c -behaviour of $r_1^{3/1}$: dot-dashed line (red) and $r_2^{3/1}$: continuous line (green) with $b = -0.35$ and $\tau = 0.6 \text{ GeV}^{-2}$.

The corresponding curves are qualitatively similar to the charm quark one. We take $b = -0.35$ like in the case of the charm quark. The τ -stability is reached for $\tau \geq 0.6 \text{ GeV}^{-2}$ as shown in Fig. 4, where we also see that $r_{12}^{3/1}$ is more affected by the mixed condensate contributions than $r_i^{3/1}$. Therefore, we shall eliminate it from our choice. Another argument raised later about the radiative corrections does not also favour $r_{12}^{3/1}$. In Fig. 4, we study the t_c -stability of $r_i^{3/1}$ which is reached for $t_c \geq 95 \text{ GeV}^2$. Within these optimal conditions, one deduces from $r_i^{3/1}$ to lowest order:

$$\frac{M_{\Xi_{bb}^*}}{M_{\Xi_{bb}}} = 1.0000. \quad (23)$$

Estimate of the $O(\alpha_s)$ corrections

Radiative corrections due to α_s are known to be large in the baryon two-point correlators [17, 41]. However, one can easily inspect that in the simple ratios \mathcal{R}_i^3 and \mathcal{R}_i^1 these huge corrections cancel out, while its only remain the one induced by the anomalous dimension of the baryon operators. Including the anomalous dimension $\gamma=2$ (resp $-2/3$) for the spin 1/2 (resp 3/2) baryons [17], one can generically write the PT expressions of the moment sum rule defined in Eq. (13) to leading order in t/m_Q^2 , which is a crude approximation but very informative:

$$\mathcal{F}_i(\tau)|_{\text{pert}} \approx (\alpha_s(\tau))^{-\frac{\gamma}{\beta_1}} A_i \tau^{-3} \left(1 + K_i \frac{\alpha_s}{\pi}\right), \quad (24)$$

where β_1 is the first coefficient of the β -function; A_i is a known LO expression; K_i is the radiative correction which is known in some cases of light and heavy baryons [17, 41]. From the previous expression in Eq. (24), one can derive the ratio of sum rules defined in Eq. (14) and then the DRSR in Eq. (18):

$$r_i^{3/1}|_{\text{pert}}^{NLO} \approx r_i^{3/1}|_{\text{pert}}^{LO} \times \left[1 + \frac{2}{9} \frac{\alpha_s}{\pi} + O(\alpha_s^2, M_Q^2 \tau)\right]. \quad (25)$$

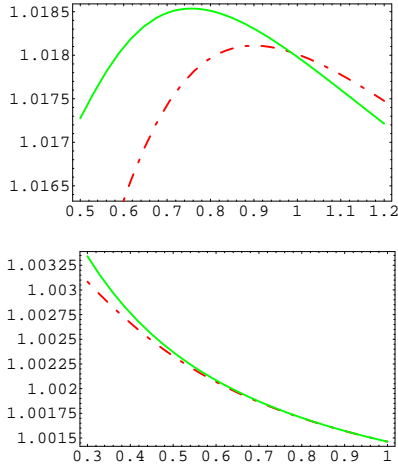


Figure 6: **Charm quark:** a) τ -behaviour of $r_1^{3/1}$: dot-dashed line (red) and $r_2^{3/1}$: continuous line (green) with $b = -0.35$, $t_c = 25 \text{ GeV}^2$ where radiative corrections have been included. **Bottom quark:** b) the same as in a) but for the bottom quark. We use $b = -0.35$ and $t_c = 100 \text{ GeV}^2$

It is important to notice for $r_i^{3/1}$ that the radiative correction has been only induced by the ones due to the anomalous dimensions, while the one due to K_i cancels out to this order. This is not the case of $r_{12}^{3/1}$ where the radiative correction is only due to $K_2 - K_1$ and needs to be evaluated which is beyond the aim of this letter. Therefore, in the following, we shall only consider the results from $r_i^{3/1}$. In our numerical analysis, we shall include the α_s correction into the complete LO expressions of the correlators. We show the τ -dependence of the DRSR in Fig. 6. We shall take the range of τ -values where the LO expressions have τ -stability which is $(0.7-1) \text{ GeV}^{-2}$ for charm and $(0.5-0.8) \text{ GeV}^{-2}$ for bottom (see Figs. 2 and 4). One can also notice that the NLO DRSR for charm presents a τ -extremum in the above range $(0.7-1) \text{ GeV}^{-2}$ of τ rendering its prediction more reliable than for the bottom channel case. We can deduce :

$$\frac{M_{\Xi_{cc}^*}}{M_{\Xi_{cc}}} = 1.0167(10)_{\alpha_s(16)_{m_c}}, \quad \frac{M_{\Xi_{bb}^*}}{M_{\Xi_{bb}}} = 1.0019(3)_{\alpha_s(2)_{m_b}}. \quad (26)$$

This would correspond to the mass-splittings (in units of MeV):

$$M_{\Xi_{cc}^*} - M_{\Xi_{cc}} = 59(7), \quad M_{\Xi_{bb}^*} - M_{\Xi_{bb}} = 19(3), \quad (27)$$

if one uses the experimental value 3.52 GeV of the Ξ_{cc} mass which agrees with the QSSR prediction in Eq. (1). For the Ξ_{bb} mass, we have used the central value 9.94 GeV in Eq. (1). The ccq mass-splitting is comparable with the one of about 70 MeV from potential models [10, 14] but larger than the one of about 24 MeV obtained in [16]. The bbq mass-splitting also agrees with potential models and seems to indicate a $1/M_b$ behaviour which is also seen on the lattice [42]. Our result excludes the possibility that $M_{\Xi_{cc}^*} \geq M_{\Xi_{cc}} + m_\pi$, indicating that it can only decay electromagnetically:

$$M_{\Xi_{cc}^*} \rightarrow M_{\Xi_{cc}} \gamma, \quad M_{\Xi_{cc}^*} \not\rightarrow M_{\Xi_{cc}} \pi. \quad (28)$$

A future discovery of the Ξ_{cc}^* and Ξ_{bb}^* can inform or support our predictions given to that order of QCD perturbative series. We consider the previous results as an improvement of the former ones deduced from the mass values in Eq. (1) obtained by [9]:

$$\frac{M_{\Xi_{cc}^*}}{M_{\Xi_{cc}}} \simeq 1.03 \pm 0.03, \quad \frac{M_{\Xi_{bb}^*}}{M_{\Xi_{bb}}} = 1.04 \pm 0.23. \quad (29)$$

6. The Ω_{cc}/Ξ_{cc} mass ratio

We use the DRSR in Eq. (18) where their QCD expressions

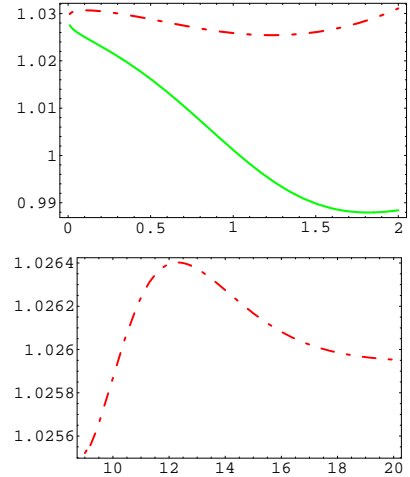


Figure 7: Ω_{cc}/Ξ_{cc} : a) τ -behaviour of $r_2^{sd}(cc)$: continuous line (green) and $r_1^{sd}(cc)$: dot-dashed line (red) in the charm quark channel for $b = -0.35$, $t_c = 12 \text{ GeV}^2$ and $m_c = 1.26 \text{ GeV}$. b) t_c -behaviour of $r_1^{sd}(cc)$ for $\tau = 1 \text{ GeV}^{-2}$: dot-dashed line (red)

can be obtained from the one of the two-point correlator in [9] and the new quark mass corrections in Eq. (10). One can also deduce from Eq. (24) that the light-flavour independent radiative corrections including the one due to the anomalous dimensions disappear in the SU(3) breaking DRSR, while the most relevant radiative corrections are the one corresponding to the m_s and $\langle \bar{s}s \rangle$ terms which are beyond the scope of the LO analysis in this paper. We show in Fig. 7a the τ -behaviour of the DRSR for $m_c = 1.26 \text{ GeV}$ and $b = -0.35$ for a given $t_c = 10 \text{ GeV}^2$. We have not shown $r_{12}^{sd}(cc)$ which is the lesser stable

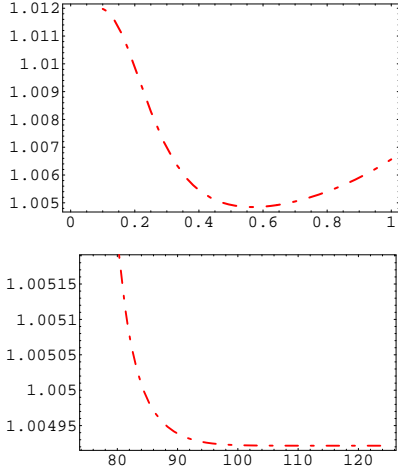


Figure 8: Ω_{bb}/Ξ_{bb} : a) τ -behaviour of $r_1^{sd}(bb)$: dot-dashed line (red) in the bottom quark channel for $b = -0.35$, $t_c = 100 \text{ GeV}^2$ and $m_b = 4.22 \text{ GeV}$. b) t_c -behaviour of $r_1^{sd}(bb)$ for $\tau = 0.5 \text{ GeV}^{-2}$: dot-dashed line (green)

among the three. We see that the most stable result is given by $r_1^{sd}(cc)$. We show in Fig. 7b the t_c -behaviour of $r_1^{sd}(cc)$ for a given $\tau = 1 \text{ GeV}^{-2}$. We deduce from the previous analysis:

$$r_1^{sd}(cc) \equiv \frac{M_{\Omega_{cc}}}{M_{\Xi_{cc}}} = 1.026(5)_{m_c}(2)_{\bar{s}s}(4)_{m_s}, \quad (30)$$

where the sub-indices indicate the different sources of errors (the parameters not mentioned induce negligible errors). This ratio corresponds to :

$$M_{\Omega_{cc}} - M_{\Xi_{cc}} = 92(24) \text{ MeV}, \quad (31)$$

where we have taken the experimental value $M_{\Xi_{cc}} \simeq 3.52 \text{ GeV}$ from [13]. The errors induced by the other parameters in Table 1 are negligible. We perform an analogous analysis in the b -channel, which we show in Fig. 8. In this case, we obtain:

$$r^{sd}(bb) \simeq 1.0049(7)_{m_b}(3)_{\bar{s}s}(10)_{m_s}, \quad (32)$$

which corresponds to:

$$M_{\Omega_{bb}} - M_{\Xi_{bb}} = 49(13) \text{ MeV}, \quad (33)$$

when we take the value $M_{\Xi_{bb}} \simeq 9.94 \text{ GeV}$ from [9]. Our results indicate an approximate decrease like $1/m_Q$ of the mass splittings from the c to the b quark channels. This behaviour can be qualitatively understood from the QCD expressions of the corresponding correlator, where the m_s corrections enter like m_s/m_Q , and which can be checked using some alternative methods.

7. The Ω_{QQ}^*/Ξ_{QQ}^* mass ratio

We pursue our analysis for the spin 3/2 baryons. The QCD expression of the ratios of moments can be obtained from the ones of the two-point correlator in [9] and the new mass corrections given in Eq. (11). Including the contributions of the dimension-4 condensates, we show your analysis in Fig. 9. One can see in Fig. 9a that r_1^{sd} and r_2^{sd} are quite stable versus τ from $\tau \geq 0.4$

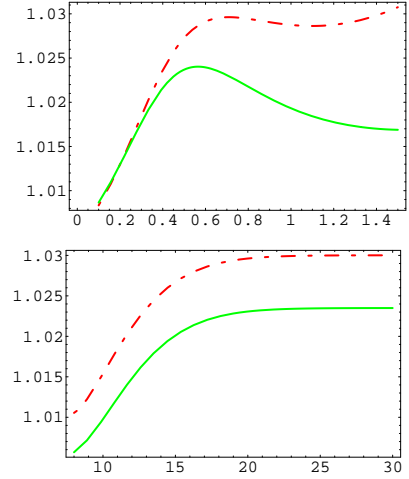


Figure 9: Ω_{cc}^*/Ξ_{cc}^* : a) τ -behaviour of $r_1^{sd}(cc)^*$: dot-dashed line (red) and $r_2^{sd}(cc)^*$: continuous line (green) in the charm quark channel for $t_c = 20 \text{ GeV}^2$ and $m_c = 1.26 \text{ GeV}$. b) t_c -behaviour of $r_1^{sd}(cc)^*$ and $r_2^{sd}(cc)^*$ for $\tau = 0.7 \text{ GeV}^{-2}$

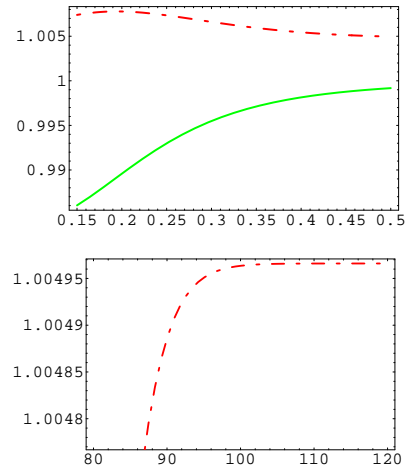


Figure 10: Ω_{bb}^*/Ξ_{bb}^* : a) τ -behaviour of $r_1^{sd}(bb)^*$: dot-dashed line (red) and of $r_2^{sd}(bc)^*$: continuous line (green) in the bottom quark channel for $t_c = 100 \text{ GeV}^2$ and $m_b = 4.22 \text{ GeV}$. b) t_c -behaviour of $r_1^{sd}(bb)^*$ for $\tau = 0.5 \text{ GeV}^{-2}$

GeV^{-2} . In Fig. 9b, we show the t_c -behaviour of r_1^{sd} and r_2^{sd} given τ . We deduce at the stability regions:

$$r^{sd}(cc)^* \equiv \frac{M_{\Omega_{cc}^*}}{M_{\Xi_{cc}^*}} = 1.026(4)_{\bar{s}s}(4)_{m_s}(6)_{m_c}(1)_{t_c}, \quad (34)$$

where the errors coming from other parameters than $\bar{s}s$ are negligible. This implies:

$$M_{\Omega_{cc}^*} - M_{\Xi_{cc}^*} = 94(27) \text{ MeV}, \quad (35)$$

where we have used $M_{\Xi_{cc}^*} \simeq 3.58 \text{ GeV}$ from Eq. (31) and the experimental value of $M_{\Xi_{cc}^*}$. We show in Fig. 10 the analogous analysis for the bottom channel. We deduce:

$$r^{sd}(bb)^* \equiv \frac{M_{\Omega_{bb}^*}}{M_{\Xi_{bb}^*}} = 1.0050(3)_{\bar{s}s}(10)_{m_s}(4)_{\tau}(10)_{m_b}, \quad (36)$$

where the error is again mainly due to $\langle \bar{s}s \rangle$, the others being negligible. This implies:

$$M_{\Omega_{bb}^*} - M_{\Xi_{bb}^*} = 50(15) \text{ MeV}, \quad (37)$$

where we have used $M_{\Xi_{bb}^*} \simeq 9.96$ GeV using our prediction in the previous section. This result agrees with the potential model one of about 60 MeV given in [10]. Again like in the case of spin 1/2 baryons, the SU(3) mass-differences appears to behave like the inverse of the heavy quark masses, which can be inspected from the QCD expressions of the two-point correlator. One can also observe that the mass-splittings are almost the same for the spin 1/2 and spin 3/2 baryons.

8. The Ω_{bc}/Ξ_{bc} mass ratio

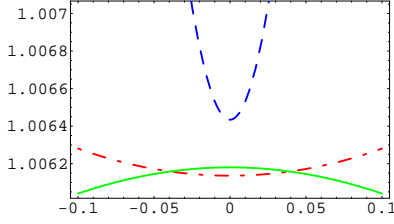


Figure 11: Ω_{bc}/Ξ_{bc} : b behaviour of $r_1^{sd}(bc)$: dot-dashed line (red); $r_2^{sd}(bc)$: continuous line (green), and $r_{12}^{sd}(bc)$: dashed line (blue) for $t_c = 50$ GeV², $\tau = 0.8$ GeV⁻², $m_c = 1.26$ GeV and $m_b = 4.22$ GeV.

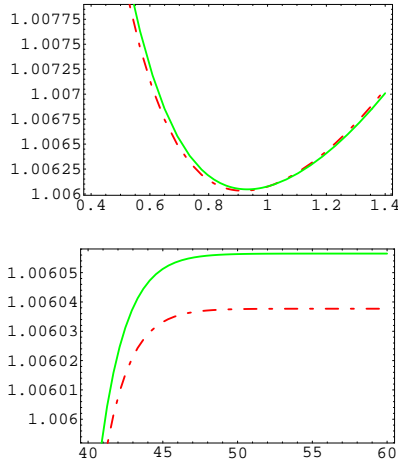


Figure 12: Ω_{bc}/Ξ_{bc} a): τ -behaviour of $r_1^{sd}(bc)$: dot-dashed line (red) and $r_2^{sd}(bc)$: continuous line (green) for $k = -0.05$, $t_c = 50$ GeV² and $m_c = 1.26$ GeV. b): t_c -behaviour of $r_1^{sd}(bc)$ and $r_2^{sd}(bc)$ for $\tau = 0.9$ GeV⁻² and $k = -0.05$.

The $\Xi(bc)$ and the $\Omega(bc)$ spin 1/2 baryons can be described by the corresponding currents:

$$\begin{aligned} J_{\Xi_{bc}} &= \epsilon_{\alpha\beta\lambda} \left[(c_\alpha^T C \gamma_5 d_\beta) + k (c_\alpha^T C d_\beta) \gamma_5 \right] b_\lambda, \\ J_{\Omega_{bc}} &= J_{\Lambda_{bc}} (d \rightarrow s), \end{aligned} \quad (38)$$

where d, s are light quark fields, c, b are heavy quark fields and k is *a priori* an arbitrary mixing parameter. The expression of the corresponding two-point correlator has been obtained in the chiral limit $m_d = m_s = 0$ by Refs. [9, 10]. We have checked these expressions which we complete here by adding the m_s -corrections for the PT and quark condensate contributions. The

expressions of these corrections are:

$$\begin{aligned} \text{Im} F_1^{m_q}|_{\text{pert}} &= -\frac{m_s m_c (1-k^2)}{128 \pi^3 t^2} \left[6 \mathcal{L}_1 [(m_c^2 t^2 - 2m_b^4 m_c^2)] \right. \\ &\quad + 6 \mathcal{L}_2 m_c^2 t^2 - \lambda_{bc} \left[2t^2 + (5m_c^2 - 4m_b^2) t \right. \\ &\quad \left. \left. - m_c^4 + 5m_b^2 m_c^2 + 2m_b^4 \right] \right] \\ \text{Im} F_1^{m_s}|_{\bar{s}s} &= \frac{m_s \mathcal{B}(1+k^2)}{32 \pi t^3} \left[\lambda_{bc} [t^2 + (m_b^2 + m_c^2) t \right. \\ &\quad - 2(m_b^2 - m_c^2)^2] + \frac{2}{\lambda_{bc}} [(m_b^4 + m_c^4) t^2 \\ &\quad \left. - 2(m_b^2 + m_c^2)(m_b^2 - m_c^2)^2 t + (m_b^2 - m_c^2)^4] \right], \end{aligned} \quad (39)$$

$$\begin{aligned} \text{Im} F_2^{m_s}|_{\text{pert}} &= -\frac{3m_s m_c m_b (1+k^2)}{64 \pi^3 t} \left[2 \mathcal{L}_1 [(m_b^2 + m_c^2) t - 2m_b^2 m_c^2] - 2 \mathcal{L}_2 (m_b^2 - m_c^2) t \right. \\ &\quad \left. - \lambda_{bc} [s + m_b^2 + m_c^2] \right] \\ \text{Im} F_2^{m_s}|_{\bar{s}s} &= \frac{m_s m_b \mathcal{B}(1-k^2)}{16 \pi t^2} \left[\lambda_{bc} (t - m_b^2 + m_c^2) + \frac{1}{\lambda_{bc}} [m_b^2 t^2 + (m_c^4 + m_b^2 m_c^2 - 2m_b^4) t \right. \\ &\quad \left. + (m_b^2 - m_c^2)^3] \right], \end{aligned} \quad (40)$$

where:

$$\begin{aligned} v &= \sqrt{1 - \frac{4m_b^2 m_c^2}{(t - m_b^2 - m_c^2)^2}}, \quad \lambda_{bc}^{1/2} = (t - m_b^2 - m_c^2) v \\ \mathcal{L}_1 &= \frac{1}{2} \log \frac{1+v}{1-v} \\ \mathcal{L}_2 &= \log \frac{(m_b^2 + m_c^2) t + (m_b^2 - m_c^2)(\lambda_{bc}^{1/2} - m_b^2 + m_c^2)}{2m_b m_c t}. \end{aligned} \quad (41)$$

Like in previous sections, we study the different ratios of moments in Figs. 11 and 12. As one can see in Fig. 11a, $r_1^{sd}(bc)$ and $r_2^{sd}(bc)$ are quite stable in k and present common solutions for :

$$k = \pm 0.05, \quad (42)$$

inside the range given in Eq. (5), while $r_{12}^{sd}(bc)$ does not intersect with the other DRSR. The τ and t_c behaviours given in Fig. 12a,b are also very stable from which we deduce the DRSR:

$$r^{sd}(bc) \equiv \frac{M_{\Omega_{bc}}}{M_{\Xi_{bc}}} = 1.006(0.2)_{\bar{s}s}(1.4)_{m_s}(1)_{m_Q}, \quad (43)$$

where the errors coming from other parameters are negligible. This implies:

$$M_{\Omega_{bc}} - M_{\Xi_{bc}} = 41(7) \text{ MeV}, \quad (44)$$

where we have used the QSSR central value $M_{\Xi_{bc}} \simeq 6.86$ GeV in Eq. (2). The size of the mass-splitting can be compared with the potential model prediction about (70-89) MeV given in [10, 15].

Table 2: QSSR predictions for the doubly heavy baryons mass ratios and splittings, which we compare with the Potential Model (PM) range of results in [10, 15]. The PM prediction for the spin 3/2 is an average with the one for spin 1/2. The mass inputs are in GeV and the mass-splittings are in MeV.

Mass ratios	Mass inputs	Mass plittings	PM
$\Xi_{cc}^*/\Xi_{cc} = 1.0167(19)$	$\Xi_{cc} = 3.52[13]$	$\Xi_{cc}^* - \Xi_{cc} = 59(7)$	70-93
$\Xi_{bb}^*/\Xi_{bb} = 1.0019(3)$	$\Xi_{bb} = 9.94[9]$	$\Xi_{bb}^* - \Xi_{bb} = 19(3)$	30-38
$\Omega_{cc}^*/\Omega_{cc} = 1.0260(70)$	$\Xi_{cc} = 3.52[13]$	$\Omega_{cc} - \Xi_{cc} = 92(24)$	90-102
$\Omega_{bb}^*/\Xi_{bb} = 1.0049(13)$	$\Xi_{bb} = 9.94[9]$	$\Omega_{bb} - \Xi_{bb} = 49(13)$	60-73
$\Omega_{cc}^*/\Xi_{cc}^* = 1.0260(75)$	$\Xi_{cc}^* = 3.58^*)$	$\Omega_{cc}^* - \Xi_{cc}^* = 94(27)$	91-100
$\Omega_{bb}^*/\Xi_{bb}^* = 1.0050(15)$	$\Xi_{bb}^* = 9.96^*)$	$\Omega_{bb}^* - \Xi_{bb}^* = 50(15)$	60-72
$\Omega_{bc}^*/\Xi_{bc} = 1.0060(17)$	$\Xi_{bc} = 6.86[10]$	$\Omega_{bc} - \Xi_{bc} = 41(7)$	70-89

^{*)} We have combined your results for the mass-splittings with the experimental value of $M_{\Xi_{cc}}$ and with the central value of $M_{\Xi_{bb}}$ in Eq. (1).

9. Conclusions

Our different results are summarized in Table 2 and agree in most cases with the potential model predictions given in [10, 14]:

- The mass-splittings between the spin 3/2 and 1/2 baryons, derived in Eqs. (22) and (23) is essentially due to the radiative corrections in our approach and seems to behave like $1/M_Q$.
- For the SU(3) mass-splittings, our results, derived in Eqs. (31) and (33) for the spin 1/2 and in Eqs. (35) and (37) for the spin 3/2, indicate that the splittings due to the SU(3) breaking are almost independent on the spin of the heavy baryons but approximately behave like $1/M_Q$. These mass-behaviours can be qualitatively understood from the QCD expressions of the corresponding correlators where the leading mass corrections behave like m_s/m_Q .
- Finally, we obtain, in Eq. (44), the SU(3) mass-splittings between the $\Omega(bcs)$ and $\Xi(bcd)$, which is about 1/2 of the potential model prediction.

Our previous predictions can improved by including radiative corrections to the SU(3) breaking terms and can be tested, in the near future, at Tevatron and LHCb.

Acknowledgements

We thank Marina Nielsen, Jean-Marc Richard and Valya Zakharov for some discussions. R.M.A acknowledges the LPTA-Montpellier for the hospitality where this work has been done. This work has been partly supported by the CNRS-IN2P3 within the Non-perturbative QCD program in Hadron Physics.

References

[1] R.M. Albuquerque, S. Narison, M. Nielsen, *Phys. Lett. B* **684** (2010) 236.
[2] S. Narison, *Phys. Lett. B* **387** (1996) 162.
[3] S. Narison, *Phys. Lett. B* **210**, 238 (1988); *Phys. Lett. B* **605**, 319 (2005).
[4] S. Narison, *Phys. Lett. B* **322** (1994) 327.
[5] S. Narison, *Phys. Lett. B* **337** (1994) 166; *Phys. Lett. B* **668** (2008) 308.
[6] S. Narison, *Phys. Rev. D* **74** (2006) 034013; *Phys. Lett. B* **358** (1995) 113; *Phys. Lett. B* **466** (1999) 34.

[7] M.A. Shifman, A.I. and Vainshtein and V.I. Zakharov, *Nucl. Phys. B* **147**, 385 (1979).
[8] For a review and references to original works, see e.g., S. Narison, *QCD as a theory of hadrons, Cambridge Monogr. Part. Phys. Nucl. Phys. Cosmol.* **17**, 1-778 (2002) [hep-h/0205006]; *QCD spectral sum rules*, *World Sci. Lect. Notes Phys.* **26**, 1-527 (1989); *Acta Phys. Pol.* **B26** (1995) 687; *Riv. Nuov. Cim.* **10N2** (1987) 1; *Phys. Rept.* **84**, 263 (1982).
[9] E. Bagan, M. Chabab and S. Narison, *Phys. Lett. B* **306** (1993) 350.
[10] E. Bagan, H.G. Dosch, P.Gosdzinsky, S. Narison and J.M. Richard, *Z. Phys. C* **64** (1994) 57.
[11] J.R Zhang and M.Q Huang, *Phys. Rev. D* **78** (2008) 094007.
[12] Z.-G. Wang, *arXiv: 1003.2838 [hep-ph]* (2010) arXiv:1002.2471 [hep-ph] (2010); arXiv:1001.4693 [hep-ph] (2010).
[13] PDG 08, C. Amsler et al., *Phys. Lett. B* **667** (2008) 1; The SELEX collaboration: A. Ocherashvili et al., *Phys. Lett. B* **628** (2005) 18; M. Mattson et al., *Phys. Rev. Lett.* **89** (2002) 112001.
[14] S. Fleck and J.M. Richard, *Prog. Theor. Phys.* **82** (1989) 760; For recent reviews, see e.g.: E. Klempf, J.M. Richard, *arXiv:arXiv:0901.2055 [hep-ph]* (to appear in *Rev. Mod. Phys.*); M. Karliner, B. Keren-Zur, J.H. Lipkin, J.L. Rosner, *arXiv:0706.2163 [hep-ph]*.
[15] B. Silvestre-Brac, *Prog. Part. Nucl. Phys.* **36** (1996) 263.
[16] J. Vijande, H. Garcilazo, A. Valcarce and R. Fernandez, *Phys. Rev. D* **70** (2004) 054022.
[17] Y. Chung et al., *Z. Phys. C* **25** (1984) 151; M. Jamin, *Z. Phys. C* **37** (1988) 635; H.G. Dosch, M. Jamin and S. Narison, *Phys. Lett. B* **220** (1989) 251; H.G. Dosch, talk given at QCD10 (25th anniversary) Montpellier.
[18] E. Bagan, M. Chabab, H.G. Dosch, S. Narison, *Phys. Lett. B* **278** (1992) 367.
[19] E. Bagan, M. Chabab, H.G. Dosch, S. Narison, *Phys. Lett. B* **287** (1992) 176.
[20] E. Bagan, M. Chabab, H.G. Dosch, S. Narison, *Phys. Lett. B* **301** (1993) 243.
[21] R.A. Bertlmann, G. Launer and E. de Rafael, *Nucl. Phys. B* **250** (1985) 61; R.A. Bertlmann et al., *Z. Phys. C* **39** (1988) 231.
[22] J. Bijnens, J. Prades and E. de Rafael, *Phys. Lett. B* **348** (1995) 253.
[23] W. Lucha, D. Melikhov and S. Simula, *Phys. Rev. D* **76** (2007) 036002.
[24] J.S. Bell and R.A. Bertlmann, *Nucl. Phys. B* **177** (1981) 218. **B187** (1981) 285; R.A. Bertlmann, *Acta Phys. Austr.* **53** (1981) 305.
[25] S. Narison, E. de Rafael, *Phys. Lett. B* **103** (1981) 57.
[26] E.G. Floratos, S. Narison and E. de Rafael, *Nucl. Phys. B* **155** (1979) 155.
[27] K. Chetyrkin, S. Narison and V.I. Zakharov, *Nucl. Phys. B* **550**, 353 (1999); For a review, see e.g. S. Narison, *Nucl. Phys. Proc. Suppl.* **164** (2007) 225; S. Narison and V.I. Zakharov, *Phys. Lett. B* **679** (2009) 355.
[28] For a review, see e.g. V.A. Zakharov, *Nucl. Phys. (Proc. Sup.) B* **74** (1999) 392; V.I. Zakharov, *Nucl. Phys. Proc. Suppl.* **164** (2007) 240.
[29] See e.g.: S. Narison, *arXiv:hep-ph 0202200*; *Phys. Lett. B* **216** (1989) 191; S. Narison, H.G. Dosch, *Phys. Lett. B* **417** (1998) 173; S. Narison, N. Paver, E. de Rafael and D. Treleani, *Nucl. Phys. B* **212** (1983) 365; S. Narison, E. de Rafael, *Phys. Lett. B* **103** (1981) 57; C. Becchi, S. Narison, E. de Rafael, F.J. Yndurain, *Z. Phys. C* **8** (1981) 335.
[30] S. Narison, *Phys. Lett. B* **104** (1981) 485; S. Narison, N. Paver and D. Treleani, *Nuov. Cim. A* **74** (1983) 347.
[31] C.A. Dominguez, N.F. Nasrallah and K. Schilcher, *JHEP* **0802** (2008) 072.
[32] S. Narison, *Phys. Lett. B* **673** (2009) 30.
[33] G. Launer, S. Narison and R. Tarrach, *Z. Phys. C* **26** (1984) 433.
[34] S. Narison, *Phys. Lett. B* **300** (1993) 293; *ibid B* **361** (1995) 121.
[35] F.J. Yndurain, hep-ph/9903457.
[36] S. Narison, *Phys. Lett. B* **387** (1996) 162.
[37] S. Narison, *arXiv:1004.5333 [hep-ph]* (2010) (Phys. Lett. B in press).
[38] E. Braaten, S. Narison and A. Pich, *Nucl. Phys. B* **373** (1992) 581.
[39] B.L. Ioffe, *Nucl. Phys. B* **188** (1981) 317, **B **191** (1981) 591; A.A.Ovchinnikov and A.A.Pivovarov, *Yad. Fiz.* **48** (1988) 1135.
[40] S. Narison, *Phys. Lett. B* **197** (1987) 405; *Phys. Lett. B* **341** (1994) 73; *Phys. Lett. B* **520** (2001) 115.
[41] A.A. Ovchinnikov, A.A. Pivovarov and L.R. Surguladze, *Int. J. Mod. Phys. A* **6** (1991) 2025; S. Groote, J.G. Korner and O.I. Yakovlev, *Eur. Phys. J. C* **58** (2008) 355.
[42] M. Papinutto, talk given at QCD 10 (25th anniversary), Montpellier.**